

See discussions, stats, and author profiles for this publication at: <https://www.researchgate.net/publication/26883296>

Double Orthogonal Sample Design Scheme and Corresponding Basic Patterns in Two-Dimensional Correlation Spectra for Probing Subtle Spectral Variations Caused by Intermolecular Inter...

ARTICLE *in* THE JOURNAL OF PHYSICAL CHEMISTRY A · OCTOBER 2009

Impact Factor: 2.69 · DOI: 10.1021/jp9005185 · Source: PubMed

CITATIONS

22

READS

20

11 AUTHORS, INCLUDING:



Kun Huang

Chinese Academy of Sciences

57 PUBLICATIONS 882 CITATIONS

[SEE PROFILE](#)



Ying Zhao

Chinese Academy of Sciences

97 PUBLICATIONS 1,136 CITATIONS

[SEE PROFILE](#)



Isao Noda

University of Delaware

350 PUBLICATIONS 9,228 CITATIONS

[SEE PROFILE](#)



Yukihiro Ozaki

Kwansei Gakuin University

916 PUBLICATIONS 17,698 CITATIONS

[SEE PROFILE](#)

Double Orthogonal Sample Design Scheme and Corresponding Basic Patterns in Two-Dimensional Correlation Spectra for Probing Subtle Spectral Variations Caused by Intermolecular Interactions

Chengfeng Zhang,^{†,‡,§} Kun Huang,[‡] Huizhen Li,^{‡,||} Jing Chen,[‡] Shaoxuan Liu,[‡] Ying Zhao,[†] Dujin Wang,[†] Yizhuang Xu,^{*,‡} Jinguang Wu,[‡] Isao Noda,[†] and Yukihiro Ozaki[#]

Beijing National Laboratory for Molecular Sciences, CAS Key Laboratory of Engineering Plastics, Joint Laboratory of Polymer Science and Materials, Institute of Chemistry, Chinese Academy of Sciences, Beijing 100190, PR China, Beijing National Laboratory for Molecular Sciences, College of Chemistry and Molecular Engineering, Peking University, Beijing 100871, PR China, Graduate School of Chinese Academy of Sciences, Beijing 100190, China, College of Chemistry and Environmental Science, Henan Normal University, Xinxiang 453007, PR China, The Procter & Gamble Company, West Chester, Ohio 45069, and Department of Chemistry, School of Science and Technology, Kwansei-Gakuin University, Sanda 669-1337, Japan

Received: January 18, 2009; Revised Manuscript Received: August 16, 2009

This paper introduces a new approach named double orthogonal sample design scheme (DOSD) to probe intermolecular interactions based on a framework of two-dimensional (2D) correlated spectroscopy. In this approach, specifically designed concentration series are selected according to the mathematical analysis on orthogonal vectors to generate useful 2D correlated spectra. As a result, the interfering portion can be completely removed from both synchronous and asynchronous spectra, and complementary information concerning intermolecular interactions can be obtained from the set of 2D spectra. A model system, where intermolecular interactions occur between two solutes in a solution, is used to investigate the behavior of 2D correlated spectra generated by using the DOSD approach. Simulation results demonstrate that the resultant spectral patterns can reflect subtle spectral variation in bandwidths, peak positions, and absorptivities brought about by intermolecular interaction, which are hardly visualized in conventional 1D spectra because of the severe band-overlapping problem. The ability to reveal a subtle variation in a characteristic peak in detail by using the DOSD approach provides a new opportunity to understand the nature of intermolecular interactions from a molecular structural point of view. Intermolecular interactions between iodine and benzene in CCl_4 solutions were investigated by using the proposed DOSD approach to prove the applicability of the DOSD method in real chemical systems.

Introduction

Two-dimensional (2D) correlation spectroscopy has gained interest among scientists in various fields during the last two decades^{1–26} since it was first proposed by Noda in the 1980s.^{1,2} The basic concept of the 2D correlation spectroscopy is to depict a correlation contour map by introducing a simple correlation analysis to a stimulated spectral fluctuation (called dynamic spectra) caused by a certain perturbation, which can be electrical, thermal, magnetic, chemical, acoustic, or mechanical stimulations. The 2D correlation spectroscopy has provided a new avenue in the field of molecular structure study by spreading an overlapped 1D spectrum in the second dimension. Subtle changes in the 1D spectrum, often buried in complicated spectral features of a real chemical system, can be visualized in terms of cross peaks in 2D correlation maps.

A notable feature of 2D correlation spectroscopy is that the cross peaks can be used to identify intermolecular interactions that are very important in many physical, chemical, and biological processes including molecular

recognition, molecular catalysis, and assembly of supramolecular architectures.^{27–36} In principle, the observation of a cross peak in a synchronous 2D correlation spectrum suggests the possible existence of inter- or intramolecular interactions among functional groups. However, interfering cross peaks due to other sources of synchronicity, such as concentration variations of solutes, also arise even if there is no intermolecular interaction. This problem makes it difficult to directly use the cross-peaks as a reliable criterion to judge whether intermolecular interaction actually occurs or not. Several efforts have been made to reduce the misleading effect of coincidental synchronization of dynamic spectral signals.² For example, several different perturbation frequencies were used to make sure that a cross peak can represent a true co-operativity of the functional groups caused by certain chemical interactions.

In our previous work, variable concentrations were adopted as an external perturbation to construct a 2D synchronous spectrum to characterize weak intermolecular interactions between different solutes in a solution.²⁵ The concentration perturbation possesses the advantage that the relationship between the perturbation and dynamic data becomes simple and can be expressed mathematically in a straightforward manner. A new approach called “orthogonal sample design (OSD) scheme” was then proposed by selecting the initial concentra-

[†] Institute of Chemistry, Chinese Academy of Sciences.

[‡] Peking University.

[§] Graduate School of Chinese Academy of Sciences.

^{||} Henan Normal University.

^{*} The Procter & Gamble Company.

[#] Kwansei-Gakuin University.

tions in a special way so that interfering cross peaks can be removed. As a result, intermolecular interactions that bring about systematic deviation from the Beer–Lambert law can be selectively characterized by cross peaks in the corresponding 2D synchronous spectrum.

Spectral variations in characteristic peaks caused by intermolecular interactions can be manifested by changes in bandwidth, peak position, and absorptivity. Different variation reflects different physical nature of the changes of molecular structure under the influence of intermolecular interactions. For example, changes in peak position suggest conformational changes of molecules; variation of absorptivity may reflect redistribution of electrons so that dipole moment of molecular changes; variation of bandwidths may be related to the change in the distribution of structure of molecular ensemble. However, various intermolecular interactions such as dipole–dipole interaction, albeit quite strong, can induce only subtle spectral changes that are often buried within complex spectral profiles. Therefore, it is quite difficult to investigate these intermolecular interactions directly by using conventional 1D spectroscopic methods.

Our previous work has demonstrated that the pattern of the cross peaks in 2D synchronous spectra generated by using the OSD approach may be used as a potential resolution enhancement tool that can reveal a subtle spectral variation caused by an intermolecular interaction.²⁶ However, a synchronous spectrum can present only one aspect of 2D correlated spectra. According to the basic properties of 2D correlation spectroscopy, asynchronous spectra possess the superior ability to enhance the spectral resolution. Thus, it is expected that the combination of 2D synchronous and asynchronous spectra provides comprehensive spectral information on spectral variation caused by intermolecular interactions.

In this paper, a double orthogonal sample design (DOSD) scheme is introduced to remove interfering cross peaks from both synchronous and asynchronous 2D spectra. Furthermore, we have performed a computer simulation on a model chemical system to study the ultimate spectral behaviors of the cross peaks in 2D synchronous and asynchronous spectra constructed by using the DOSD approach under different spectral variations in a 1D spectrum. Rich and complex patterns can be obtained from both the synchronous and asynchronous 2D spectra generated by using the DOSD approach. A real chemical system (iodine–benzene in CCl_4 solutions) was also investigated to prove the applicability of the proposed DOSD method.

Theory

In this paper, we use a model to explain how the DOSD approach is utilized to characterize intermolecular interactions. The model system is composed of a series of solutions ($i = 1, 2, \dots, m$) containing solutes P and Q. We adopt variable initial concentrations of P and Q as an external perturbation to generate 2D correlation spectra. This approach provides an opportunity to tailor the information content of the 2D synchronous spectra by designing suitable concentration series.

To simplify the model, we assume that P and Q exhibit characteristic peaks at spectral coordinates x and y , respectively, and the characteristic peaks of P and Q are not overlapped. In addition, the contributions from the solvent to the two characteristic peaks mentioned above do not occur. Thus, the dynamic absorbance of P and Q at x and y can be expressed as

$$\tilde{A}^i(x) = \varepsilon_P(x)L\tilde{C}_P^i - \tilde{\delta}_P^i(x) \quad (1a)$$

$$\tilde{A}^i(y) = \varepsilon_Q(y)L\tilde{C}_Q^i - \tilde{\delta}_Q^i(y) \quad (1b)$$

where ε_P and ε_Q are the molar absorptivities of the P and Q, respectively, L is the path length of the solution, and $\tilde{\delta}_P^i(x)$ and $\tilde{\delta}_Q^i(y)$ are the deviation terms from the Beer–Lambert's law, which reflect the intermolecular interactions between P and Q. \tilde{C}_P^i and \tilde{C}_Q^i are the so-called dynamic concentrations and are obtained by the following equation (eq 2).

$$\begin{aligned} \tilde{C}_P^i &= C_P^i - \bar{C}_P \\ \tilde{C}_Q^i &= C_Q^i - \bar{C}_Q \end{aligned} \quad (2)$$

where C_P^i and C_Q^i are the initial concentrations of P and Q in the i th solutions, respectively, \bar{C}_P and \bar{C}_Q are the average concentrations of P and Q over the m samples.

Subsequently, we adopt the Noda's approach to construct 2D synchronous and asynchronous spectra according to eqs 3a and 3b:⁴

$$\Phi(x,y) = \frac{1}{m-1} \sum_{i=1}^m \tilde{A}^i(x)\tilde{A}^i(y) \quad (3a)$$

$$\Psi(x,y) = \frac{1}{m-1} \sum_{i=1}^m \tilde{A}^i(x)N\tilde{A}^i(y) \quad (3b)$$

where N is the Hilbert–Noda transformation matrix.

After eq 1a is substituted into eq 3a, the intensities of cross peaks in synchronous spectra can be divided into two parts (eq 4a).

$$\Phi(x,y) = \Phi_1(x,y) + \Phi_2(x,y) \quad (4a)$$

Similarly, the intensities of cross peaks in asynchronous spectra can also be divided into two parts (eq 4b).

$$\Psi(x,y) = \Psi_1(x,y) + \Psi_2(x,y) \quad (4b)$$

$\Phi_1(x,y)$, $\Phi_2(x,y)$, $\Psi_1(x,y)$, and $\Psi_2(x,y)$ can be expressed in eqs 5a–5d

$$\begin{aligned} \Phi_1(x,y) &= -\frac{1}{m-1} \sum_{i=1}^m [\varepsilon_P(x)L\tilde{C}_P^i\tilde{\delta}_Q^i(y) + \\ &\quad \varepsilon_Q(y)L\tilde{C}_Q^i\tilde{\delta}_P^i(x) - \tilde{\delta}_P^i(x)\tilde{\delta}_Q^i(y)] \end{aligned} \quad (5a)$$

$$\Psi_1(x,y) = -\frac{1}{m-1} \sum_{i=1}^m [\varepsilon_P(x)L\tilde{C}_P^iN\tilde{\delta}_Q^i(y) + \varepsilon_Q(y)L\tilde{\delta}_P^i(x)N\tilde{C}_Q^i - \tilde{\delta}_P^i(x)N\tilde{\delta}_Q^i(y)] \quad (5b)$$

$$\Phi_2(x,y) = \frac{\varepsilon_P(x)\varepsilon_Q(y)L^2}{m-1}\tilde{C}_P \cdot \tilde{C}_Q \quad (5c)$$

$$\Psi_2(x,y) = \frac{\varepsilon_P(x)\varepsilon_Q(y)L^2}{m-1}\tilde{C}_P \cdot \tilde{C}_R \quad (5d)$$

where

$$\tilde{C}_P = \{\tilde{C}_P^1, \tilde{C}_P^2, \dots, \tilde{C}_P^m\} \quad (6a)$$

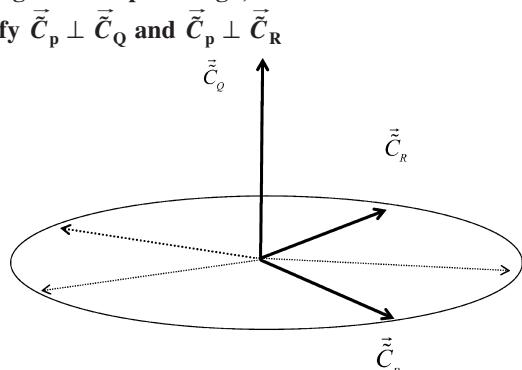
$$\tilde{C}_Q = \{\tilde{C}_Q^1, \tilde{C}_Q^2, \dots, \tilde{C}_Q^m\} \quad (6b)$$

$$\tilde{C}_R = N\tilde{C}_Q \quad (6c)$$

Since both $\Phi_1(x,y)$ and $\Psi_1(x,y)$ contain the excess terms, $\tilde{\delta}_P^i(x)$ and $\tilde{\delta}_Q^i(y)$, they reflect the intermolecular interactions in the form of the deviation from the Beer–Lambert law. On the other hand, $\Phi_2(x,y)$ and $\Psi_2(x,y)$ are just related to the concentration series of the solutes and have nothing to do with the intermolecular interactions between P and Q.

To detect intermolecular interactions by using the cross peaks in both synchronous and asynchronous spectra in a straightforward manner, a design scheme for preparing solution samples may be introduced to make $\Phi_2(x,y)$ and $\Psi_2(x,y)$ equal to zero. According to eqs 5c and eq 5d, $\Phi_2(x,y)$ and $\Psi_2(x,y)$ can be expressed in the form of dot products of two vectors. A feasible way to remove $\Phi_2(x,y)$ and $\Psi_2(x,y)$ in a nontrivial manner is that we design the dynamic concentration vectors properly, so that the vectors in eq 5c and eq 5d are orthogonal to each other. That is, \tilde{C}_P is set to be orthogonal to both \tilde{C}_Q and \tilde{C}_R . Furthermore, \tilde{C}_Q is orthogonal to \tilde{C}_R based on the property of the Hilbert–Noda transformation. The relationship among \tilde{C}_P , \tilde{C}_Q , and \tilde{C}_R is depicted in Scheme 1 and can be expressed mathematically as eq 7a and 7b. Thus, we call this approach as double orthogonal sample design (DOSD) scheme.

SCHEME 1: Schematic Diagram for the Double Orthogonal Sample Design, Where the Three Vectors Satisfy $\tilde{C}_P \perp \tilde{C}_Q$ and $\tilde{C}_P \perp \tilde{C}_R$



$$\tilde{C}_P \cdot \tilde{C}_Q = 0 \quad (7a)$$

$$\tilde{C}_P \cdot \tilde{C}_R = 0 \quad (7b)$$

Two additional requirements should be satisfied for selection of suitable dynamic concentration series of P and Q according to the basic property of dynamic concentration.

$$\sum_{i=1}^m \tilde{C}_P^i = 0 \quad (7c)$$

$$\sum_{i=1}^m \tilde{C}_Q^i = 0 \quad (7d)$$

In the following section, we term “requirement of double orthogonal sample design scheme” as the selection criterion for initial concentrations of the solutes from which the resulting dynamic concentrations satisfy eqs 7a–7d.

From a geometric point of view, at least three solution mixtures are needed to satisfy the above orthogonal requirement among the three vectors. However, it can be shown that only three solution mixtures are not enough to meet the requirement of DOSD scheme. The minimum dimension of concentration vectors turned out to be four. An example for concentration series satisfying the requirement is shown in Table 1.

Experimental Section

1. Model System. The simulated chemical system studied here consists of a series of solutions containing two chemical species P and Q. All the spectral features of the characteristic bands for P and Q, including bandwidths (W_P and W_Q), peak positions (X_P and X_Q), and absorptivities (ε_P and ε_Q) are set as listed in Table 2.

To model intermolecular interactions between P and Q in the solutions, we assume that parts of P and Q convert into a new set of chemical species U and V, respectively, thereby leading to a systematic deviation from the Beer–Lambert law. This deviation could be specified in terms of the following equilibrium shown in eq 8. From a thermodynamics point of view, the strength of intermolecular interaction can be characterized by the equilibrium constant K .

TABLE 1: Initial Concentrations of the Chemical Species P and Q in the Model System, Which Meet the Requirement of DOSD Approach

Index of the solutions	C_P (mol/dm ³)	C_Q (mol/dm ³)
1	14.00	3.55
2	16.00	19.80
3	10.00	3.35
4	0.00	13.30

TABLE 2: Spectral Variable of Species P and Q in the Model System

spectral variable	peak position (cm ⁻¹)	bandwidth (cm ⁻¹)	absorptivity
P	150	20	1.0
Q	350	20	1.0



Each trace of simulated 1D spectrum is thus the summation of the peak function of each chemical species that occurs in the solution, as shown in eq 9

$$G^i(\nu) = \sum_j \varepsilon_j L C_j^i e^{-\ln 2[(\nu - x_j)^2 / w_j^2]} \quad (9)$$

where i is the index of the solution, j corresponds to the index of chemical species (P, Q, or U, V), ν is the spectral variable, L is the path-length and set as 1 for convenience in this study, W_j , X_j , and ε_j are the bandwidth, peak position, and absorptivity of the characteristic band of the j th chemical species. C_j^i is the equilibrium concentration of the j th chemical species for the i th solution, which can be calculated by the initial concentrations of P and Q listed in Table 1 and the equilibrium constant K .

In the studies of the simulated model system, the 1D simulated spectrum for each solution with designed concentrations of different chemical species was generated by using a program written in our lab by using Turbo C 2.0. The 2D synchronous and asynchronous spectra in simulation study and the following real chemical system were all calculated by using the software of MATLAB (The Math Works Inc.). In each synchronous and asynchronous spectrum, red means the sign of the spectrum is positive, while blue means negative.

2. Real Chemical System. Iodine, AR grade, was purchased from Beijing Chemical Reagent Co. (Beijing, China). Benzene, AR grade, was purchased from Yili Fine Chemistry Co. (Beijing, China). CCl_4 (purity: >99.8%) was purchased from Chongxi Scientific Co. (Beijing, China).

Four CCl_4 solutions containing benzene and iodine were prepared. The concentrations of benzene and iodine were carefully designed according to DOSD approach as summarized in Table 3. UV-vis spectra for the solutions were recorded on a Perkin-Elmer Lambda 35 spectrometer. FT-IR spectra were measured on a Thermo-Fischer Nicolet iN10 MX spectrometer using a BaF_2 cell with a fixed spacing ($100 \mu m$). All the FT-IR spectra were obtained at a resolution of 4 cm^{-1} and 32 scans were coadded.

CCl_4 solutions with only benzene or iodine as a solute were also prepared according to the concentration series in Table 3. FT-IR spectra of benzene/ CCl_4 solutions and UV-vis spectra of iodine/ CCl_4 solutions were measured. Good linear relationships between the concentrations and the absorbance of characteristic peaks in FT-IR spectra and UV-vis spectra could be obtained (see the Supporting Information). The results demonstrate that the influence of intermolecular interactions among different benzene molecules or different iodine molecules is insignificant.

Results and Discussion

1. Role of DOSD in Eliminating Interfering Cross Peaks in 2D Synchronous and Asynchronous Spectra. First, we simulate a chemical system where no intermolecular interaction occurs between P and Q, which could be achieved by setting the equilibrium constant K as zero. As a result, only P and Q exist whereas new species U and V do not occur in the solutions. Four solutions, where the initial concentrations of P and Q meet the requirement of DOSD approach as summarized in Table 1, were selected to construct 2D synchronous and asynchronous

TABLE 3: Four Solutions in Which the Initial Concentrations of Benzene and Iodine Satisfy the DOSD Approach

solution	concentration of iodine (mg/mL)	concentration of benzene (v/v %)
1	0.60	6.3
2	3.85	7.2
3	0.56	4.5
4	2.55	0

TABLE 4: Example for Randomly Selected Concentrations of the Species P and Q in the Model System

index of the solutions	C_P (mol/dm ³)	C_Q (mol/dm ³)
1	12.00	4.00
2	10.00	10.00
3	8.00	10.00
4	10.00	16.00

spectra. The resultant 2D synchronous and asynchronous spectra are shown in Figure 1a,b. No cross peak can be observed in either synchronous or asynchronous spectra. Only autopeaks are left in the synchronous spectra, while no peak is observable in the 2D asynchronous spectra. For comparison, a randomly selected nonorthogonal concentration series as shown in Table 4 were used to construct the 2D synchronous and asynchronous spectra (Figure 1c,d) when the equilibrium constant K is again set to be zero. In these cases, interfering cross peaks develop even if no intermolecular interactions occur between P and Q (Figure 1c,d).

The above results demonstrate that the DOSD approach can remove concentration-related interfering peaks from both synchronous and asynchronous spectra successfully. This feature provides a good opportunity to study spectral variation caused by intermolecular interactions in detail.

In the following part, we study the chemical system where weak intermolecular interactions occur between species P and Q. The equilibrium constant K in eq 8 is arbitrarily set as 0.01. In this case, only a small fraction of P, Q is converted into new species U and V. That is to say, the characteristic bands of P, Q, U, and V coexist in the simulated 1D spectra. The results show that the patterns in 2D synchronous and asynchronous spectra can be used to reveal the subtle spectral variation caused by the intermolecular interactions.

2. Basic Spectral Patterns in Synchronous and Asynchronous Spectra. Here we examine the behaviors of the cross peaks in both synchronous and asynchronous spectra generated by using DOSD approach as a consequence of the variation of the spectral parameters.

The cross peaks in both synchronous and asynchronous spectrum can be divided into four spectral domains, as shown in Scheme 2. The cross peaks in domains I and IV of both synchronous and asynchronous spectra can be used to detect the intermolecular interactions between P and Q. The cross peaks in domain II reflect spectral variations of P and U, while the cross peaks in domain III are related to the spectral variation of Q and V. Cross peaks in domain I and those in domain IV are symmetric about the diagonal in 2D synchronous spectra but antisymmetric in 2D asynchronous spectra. In most cases, only the cross peaks in domain I are discussed. In synchronous spectra, domains II and III are invariantly occupied by positive autopeaks and will not be discussed further. Each cross peak in a 2D spectrum is denoted as $P_k(x,y)$ where x and y are the horizontal and vertical coordinates of the cross peak.

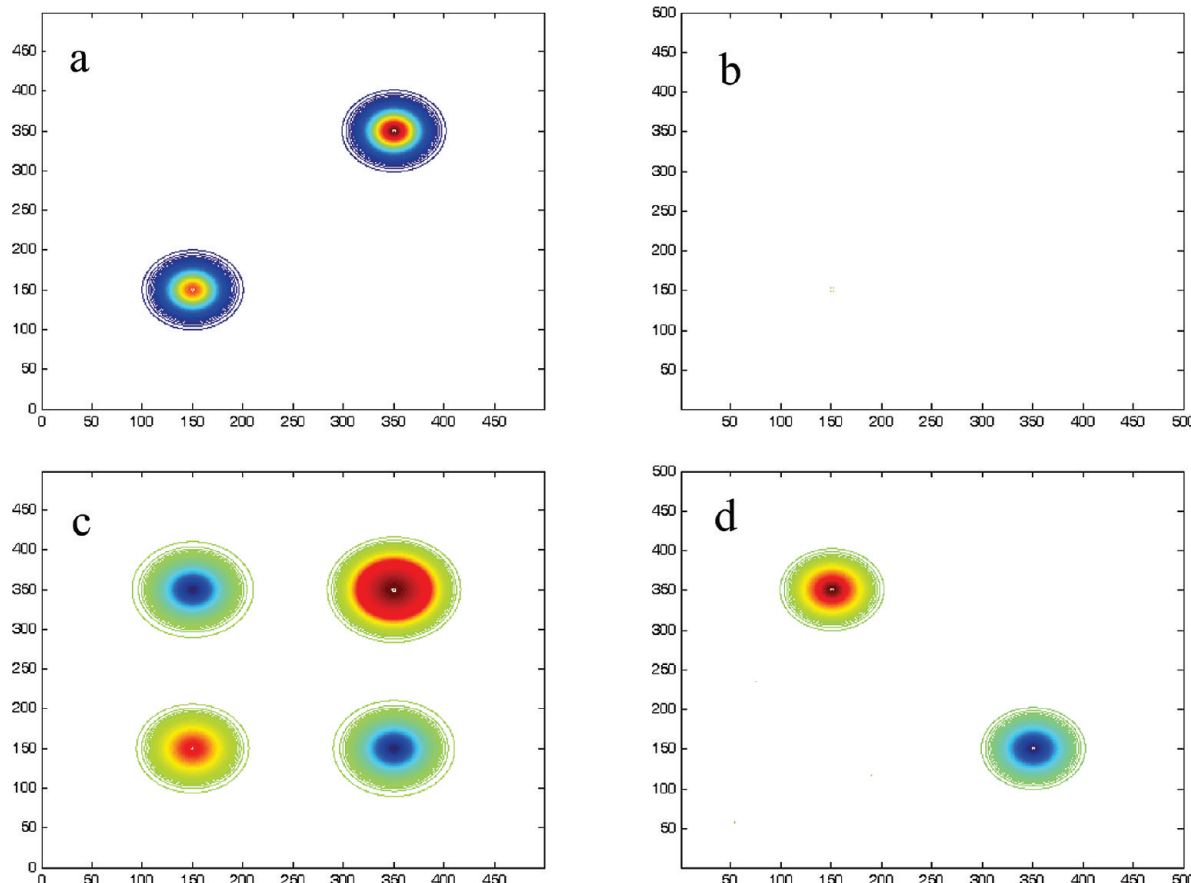
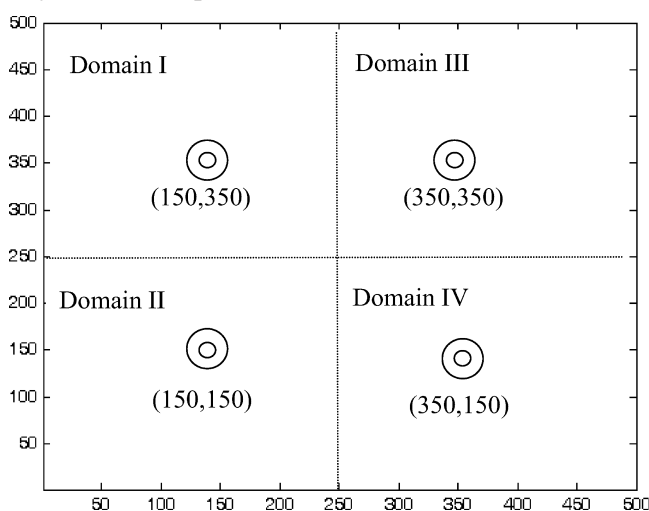


Figure 1. Simulated 2D spectra of the model system without intermolecular interactions ($K = 0$): (a) synchronous spectrum generated by DOSD approach; (b) asynchronous spectrum generated by DOSD approach; (c) synchronous spectrum generated by randomly selected concentrations; (d) asynchronous spectrum generated by randomly selected concentrations.

SCHEME 2: Schematic Diagram of the 2D Spectra, Where the Contour Map Was Divided into Four Spectral Domains in Both Synchronous and Asynchronous Spectra



The variation of the characteristic peaks of U and V can be classified into three types: bandwidth, peak position, and absorptivity. In the following section, only one type of the spectral parameters is allowed to be variable, while other types of parameters remain unchanged. The resultant 2D spectra are systematically investigated.

(1) **Effect of the Variation in Bandwidth of U and V.** The spectral variable including bandwidths, peak positions, and

TABLE 5: Spectral Variables of the Chemical Species P, Q, U, and V in the Model System Where the Bandwidths of U and V (W_U and W_V) Are Variable

spectral variable	peak position (cm ⁻¹)	bandwidth (cm ⁻¹)	absorptivity
P	150	20	1.0
Q	350	20	1.0
U	150	W_U	1.0
V	350	W_V	1.0

absorptivities for species P, Q, U, and V are summarized in Table 5. In this case, the absorptivities and peak positions of U and V are the same as those of P and Q, while the bandwidths of U and V are allowed to be changed. Here the difference in the bandwidths between P and U is denoted as ΔW_P :

$$\Delta W_P = W_U - W_P$$

Similarly, the difference in the bandwidth between Q and V is denoted as ΔW_Q :

$$\Delta W_Q = W_V - W_Q$$

Since the peak position of U is fixed to be the same as P, complete band overlapping occurs between P and U in the resultant 1D spectrum as shown in Figure 2. The resultant spectrum of mixture of P and U (Figure 2a) looks almost the same as the spectrum of P without intermolecular interactions (Figure 2b, achieved by setting the equilibrium

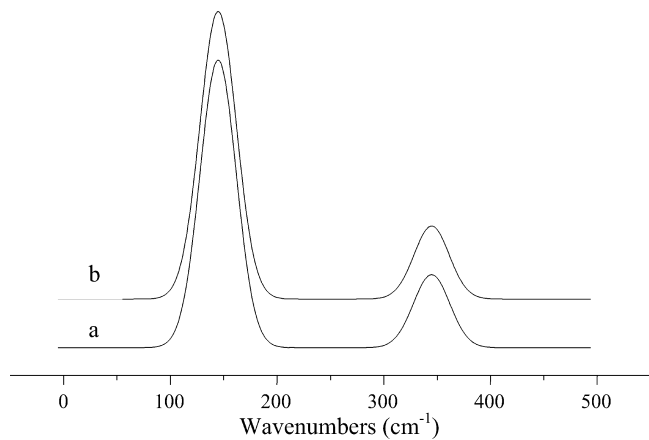


Figure 2. 1D spectra of first solution in Table 1 of the model system: (a) mixture of P, Q, U, and V since bandwidth variation is allowed due to intermolecular interactions ($W_U = 22$, $W_V = 17$); (b) no intermolecular interaction achieved by setting the equilibrium constant K to zero.

constant K zero). Only a small fraction of P converts into U and the characteristic peak of U is completely buried in the corresponding peak of P. Similar problems occur between Q and V. It is difficult to judge whether intermolecular interactions that produce new substances U and V occur or not from the conventional 1D spectra.

However, the cross peaks in 2D synchronous and asynchronous spectra generated by using the DOSD approach manage

to identify the existence of U or V caused by the intermolecular interactions. In addition, further information concerning the bandwidth variation of U and V could be retrieved on the basis of the patterns of the cross peaks.

The variation of the bandwidth of P, Q, U, and V can be classified into 9 cases. The resultant synchronous and asynchronous spectra are illustrated in Figure 3 and Figure 4 and summarized in Table 6.

In domain I of synchronous and asynchronous 2D spectra, there are three different kinds of cross peaks related to the corresponding bandwidth variations of P, Q, U, and V.

Double Cross Peaks (Figure 3b,c,d,g and Figure 4b,c,d,g). The double cross peaks appearing in domain I could be aligned in either horizontal or vertical positions:

(A) When $\Delta W_P \neq 0$ and $\Delta W_Q = 0$, horizontal double cross peaks ($Pk(150 - \delta_P, 350)$, $Pk(150 + \delta_P, 350)$) appear in domain I (Figure 3b,c and Figure 4b,c), where the value of δ_P is related to ΔW_P and will be discussed later. These two cross peaks are symmetric about the line $x = 150$. When $\Delta W_P > 0$, the cross peak in both synchronous and asynchronous spectra are positive (Figure 3b and 4b). When $\Delta W_P < 0$, the signs of the cross peaks in both synchronous and asynchronous spectra become negative (Figures 3c and 4c).

(B) When $\Delta W_P = 0$ and $\Delta W_Q \neq 0$, vertical double cross peaks ($Pk(150, 350 - \delta_Q)$, $Pk(150, 350 + \delta_Q)$) appear in domain I (Figure 3d,g and Figure 4d,g), where the value of δ_Q is related to ΔW_Q and will be discussed later. The two cross peaks are symmetric about the line $y = 350$. When $\Delta W_Q > 0$, the double

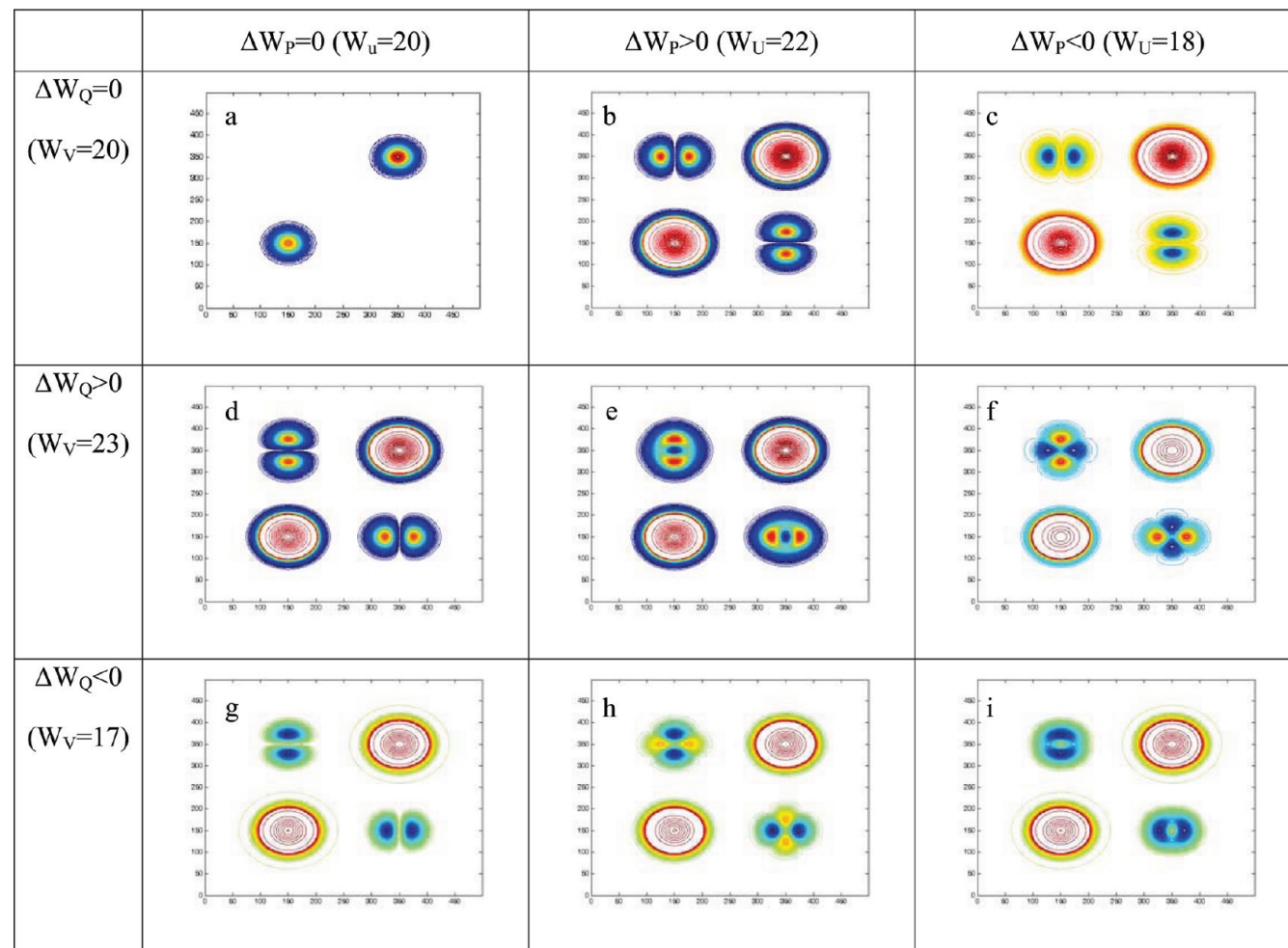


Figure 3. 2D synchronous spectra of the model system obtained as a consequence of bandwidth variations.

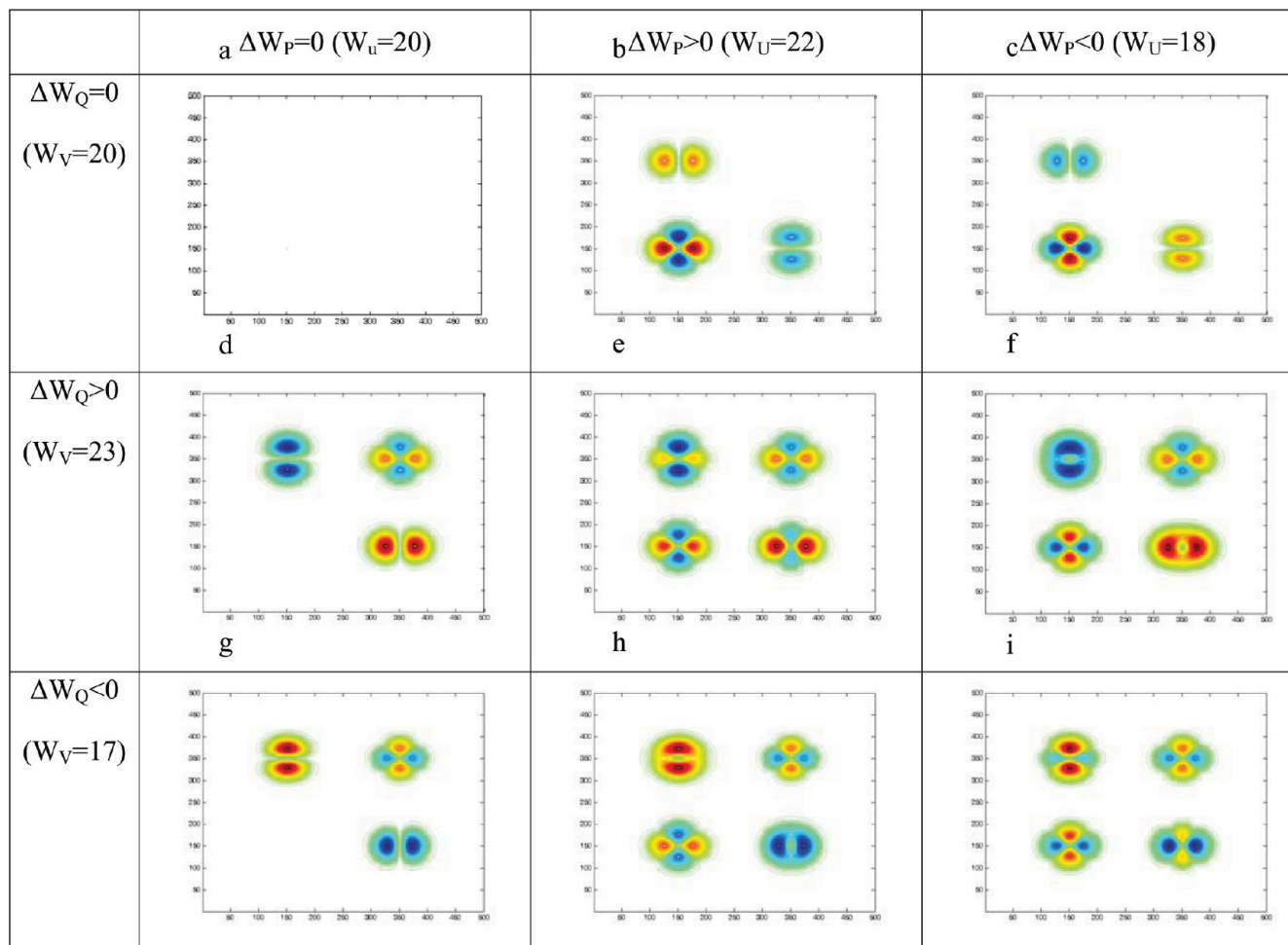


Figure 4. 2D asynchronous spectra of the model system obtained as a consequence of bandwidth variations.

cross peaks are positive in synchronous spectra (Figure 3d) but negative in asynchronous spectra (Figure 4d). When $\Delta W_Q < 0$, the signs of the cross peaks in both synchronous and asynchronous spectra are reversed (Figures 3g and 4g).

Crater-Shape (Figure 3e,i, and Figure 4f,h) and Diamond-Shape Cross Peaks (Figure 3f,h and Figure 4e,i). Two new spectral patterns, namely the diamond and the crater pattern, may appear in domain I of synchronous and asynchronous spectra. Figure 5 shows the 3D mesh plots of the crater-shape cross peaks and their behaviors upon the variation of W_u and W_v . The pattern may be a perfect crater without any peak or a crater with a pair of strong peaks along vertical or horizontal direction. It turns out that the crater is composed of a pair of vertical and a pair of horizontal cross peaks with the same sign. The overlapping of the adjacent peaks makes it difficult to identify individual peak from the peak group. However, the relative intensities of the horizontal and vertical peaks change upon variation of W_u and W_v . When the absolute intensities of the horizontal peaks are stronger than the vertical ones, two horizontal cross peaks appear on the crater as shown in Figure 5a. When the intensities of the horizontal cross peaks are roughly the same as the vertical ones, a perfect crater appears as shown in Figure 5b. The vertical cross peaks appear on the crater in Figure 5c as the absolute intensities of the vertical cross peaks become stronger.

The diamond-shape cross peaks are composed of a pair of horizontal cross peaks and a pair of vertical cross peaks, where the signs of the vertical peaks and the horizontal ones are

reversed. The reversed signs of the horizontal and vertical cross peaks preclude the possibility of overlapping among adjacent cross peaks. As a result, the four peaks are well resolved. The horizontal peaks ($Pk(150 - \delta_p, 350)$, $Pk(150 + \delta_p, 350)$) are symmetric about the line $x = 150$, while the two vertical cross peaks ($Pk(150, 350 - \delta_q)$, $Pk(150, 350 + \delta_q)$) are symmetric about the line $y = 350$. The values of δ_p and δ_q as mentioned above are related to ΔW_p and ΔW_q , respectively.

The spectral behaviors in domain II are only related to the variation of W_p and W_u and can be classified into two types. If $\Delta W_p \neq 0$, the resultant cross peaks form a diamond-shape structure (Figure 3b,c,e,f,h,i and Figure 4b,c,e,f,h,i), which consists of a pair of horizontal cross peaks ($Pk(150 - \delta_p, 150)$, $Pk(150 + \delta_p, 150)$) and a pair of vertical ones ($Pk(150, 150 - \delta_p)$, $Pk(150, 150 + \delta_p)$). The value of δ_p is related to ΔW_p and will be discussed later. When $\Delta W_p > 0$, the horizontal cross peaks are positive and the vertical ones are negative. When $\Delta W_p < 0$, the signs of the four cross peaks are all reversed. The horizontal cross peaks are symmetric about the line $x = 150$, while the vertical cross peaks are symmetric about the line $y = 150$. In addition, the four peaks distribute antisymmetrically along the diagonal line. Thus the absolute intensities of the four cross peaks are identical. If $\Delta W_p = 0$, no cross peak appears in domain II (Figure 3d, g and Figure 4d,g).

The spectral behaviors of domain III, which are only related to the variation of W_q and W_v , is very similar to that of domain II. When $W_v \neq W_q$, four peaks ($Pk(350 - \delta_q, 350)$, $Pk(350 + \delta_q, 350)$) ($Pk(350, 350 - \delta_q)$, $Pk(350, 350 + \delta_q)$) can be

TABLE 6: Synchronous and Asynchronous Spectra of the Model System As a Consequence of Bandwidth Variations (9 Cases) and the Corresponding Spectral Features in Domain I of Synchronous Spectra and Domains I, II, and III of Asynchronous Spectra^a

bandwidth variation (cm^{-1})	synchronous spectra	spectral feature of synchronous spectra (domain I)	asynchronous spectra	spectral feature of asynchronous spectra		
				domain I	domain II	domain III
(1) $\Delta W_p=0, \Delta W_q=0$ ($W_u=20, W_v=20$)	Figure 3a	none	Figure 4a	none	none	none
(2) $\Delta W_p>0, \Delta W_q=0$ ($W_u=22, W_v=20$)	Figure 3b	double cross peaks, horizontal, positive	Figure 4b	double cross peaks, horizontal, positive	diamond-shape cross peak with the horizontal part positive	none
(3) $\Delta W_p<0, \Delta W_q=0$ ($W_u=18, W_v=20$)	Figure 3c	double cross peaks, horizontal, negative	Figure 4c	double cross peaks, horizontal, negative	diamond-shape cross peak with the horizontal part negative	none
(4) $\Delta W_p=0, \Delta W_q>0$ ($W_u=20, W_v=23$)	Figure 3d	double cross peaks, vertical, positive	Figure 4d	double cross peaks, vertical, negative	none	diamond-shape cross peak with the horizontal part positive
(5) $\Delta W_p=0, \Delta W_q<0$ ($W_u=20, W_v=17$)	Figure 3g	double cross peaks, vertical, negative	Figure 4g	double cross peaks, vertical, positive	none	diamond-shape cross peak with the horizontal part negative
(6) $\Delta W_p>0, \Delta W_q>0$ ($W_u=22, W_v=23$)	Figure 3e	crater-shape cross peaks, positive	Figure 4e	diamond-shape cross peak with the horizontal part positive	diamond-shape cross peak with the horizontal part positive	diamond-shape cross peak with the horizontal part positive
(7) $\Delta W_p>0, \Delta W_q<0$ ($W_u=22, W_v=17$)	Figure 3h	diamond-shape cross peak with the horizontal part positive	Figure 4h	crater-shape cross peaks, positive	diamond-shape cross peak with the horizontal part positive	diamond-shape cross peak with the horizontal part positive
(8) $\Delta W_p<0, \Delta W_q<0$ ($W_u=18, W_v=17$)	Figure 3i	crater-shape cross peaks, negative	Figure 4i	diamond-shape cross peak with the horizontal part negative	diamond-shape cross peak with the horizontal part negative	diamond-shape cross peak with the horizontal part negative
(9) $\Delta W_p<0, \Delta W_q>0$ ($W_u=18, W_v=23$)	Figure 3f	diamond-shape cross peak with the horizontal part negative	Figure 4f	crater-shape cross peaks, negative	diamond-shape cross peak with the horizontal part negative	diamond-shape cross peak with the horizontal part positive

^a More detailed pictures for 2D spectra are shown in Figure 3.

observed, where the value of δ_Q is related to ΔW_Q and will be discussed later.

Subsequently, a systematic investigation has been performed to study the relationships between bandwidth variation of P, Q, U, and V and the resulting 2D synchronous and asynchronous spectra generated by using DOSD approach. All the spectral behaviors are similar to those shown in Figures 3 and 4 and no new spectral patterns are observed. Therefore, a one-to-one correspondence relationship can be established between the spectra patterns in synchronous as well as asynchronous spectra and the type of variation of bandwidth of U and V. Thus, the variation of U and V can be determined by the patterns of the cross peaks in

synchronous and asynchronous spectra as shown in Figure 3 and summarized in Table 6.

Moreover, quantitative judgments of W_U (ΔW_P) can also be achieved since a monotonic relationship between ΔW_P and the value of δ_P can be clearly observed as shown in Figure 6. A similar monotonic relationship also occurs between the value of δ_Q and ΔW_Q . Thus exact values of W_U and W_V can be determined from both synchronous and asynchronous spectra.

(2) Effect of the Variation in Peak Positions of U and V. In this case, the peak positions of U and V are allowed to be changed, while the absorptivities and the bandwidths of U and V are the same as those of P and Q. All the spectral variables for P, Q, U,

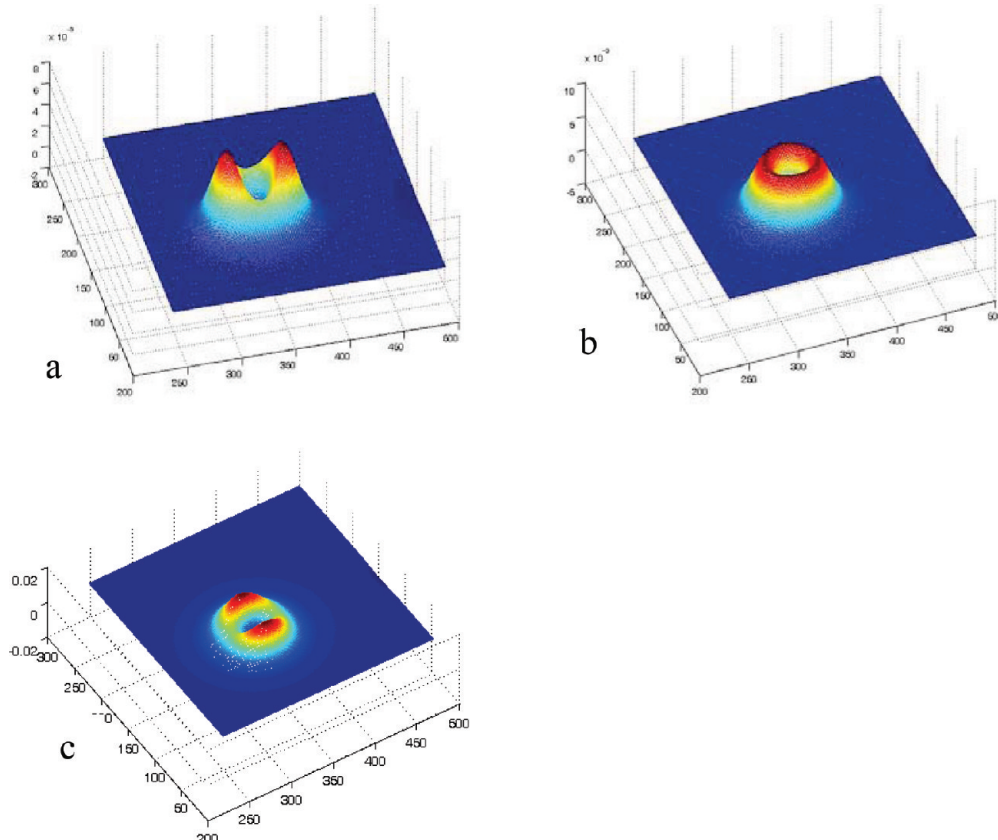


Figure 5. 3D mesh plot of the crater-shape cross peaks in domain I of the asynchronous spectra upon the variation of W_U and W_V : (a) $W_U = 22$, $W_V = 19.5$; (b) $W_U = 22$, $W_V = 19$; (c) $W_U = 22$, $W_V = 18$.

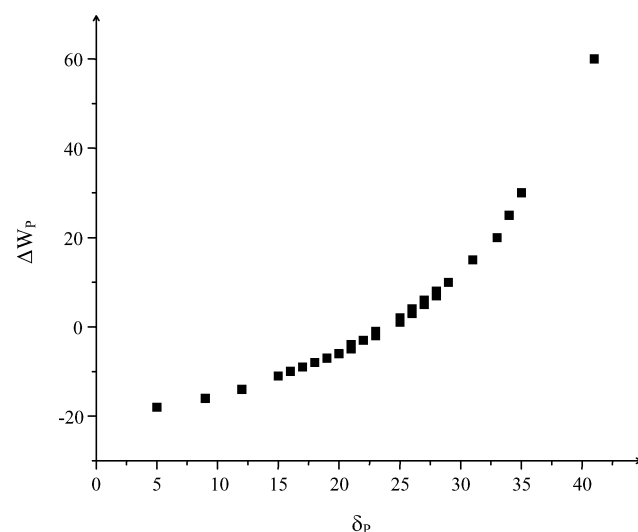


Figure 6. Monotonic relationship between ΔW_P and the value of δ_P .

and V are summarized in Table 7. The difference in the peak position between P and U is denoted as ΔX_P :

$$\Delta X_P = X_U - X_P$$

Similarly, the difference in the peak position between Q and V is denoted as ΔX_Q :

$$\Delta X_Q = X_V - X_Q$$

TABLE 7: Spectral Variables of P, Q, U, and V of the Model System Where the Peak Positions of U and V (X_U and X_V) Are Variable

spectral variable	peak position (cm^{-1})	bandwidth (cm^{-1})	absorptivity
P	150	20	1.0
Q	350	20	1.0
U	X_U	20	1.0
V	X_V	20	1.0

In many cases, severe overlapping may occur between P and U in the resultant spectra. In addition, only a small fraction of P converts into U. Thus, the characteristic peak of U is usually completely masked by the corresponding peak of P. The band overlapping is so severe that the characteristic peaks of U can be hardly found even though resolution enhancement techniques such as second derivative spectra are utilized (Figure 7). Similar problems occur between Q and V. Thus, it becomes very difficult to identify the existence of U and V from conventional 1D spectrum.

However, the cross peaks in 2D synchronous and 2D asynchronous spectra generated by using the DOSRD approach can be used to identify the existence of U or V caused by intermolecular interactions. In addition, further information concerning the peak position variation of U and V could be retrieved on the basis of the patterns of the cross peaks.

The variation of the peak positions of P, Q, U, and V can also be classified into 9 cases. The corresponding 2D synchronous and asynchronous spectra are illustrated in Figures 8 and 9 as a consequence of variation of the peak positions. Cross peak clusters, which are composed of a positive peak ($\text{Pk}(x_1, y_1)$) and a negative one ($\text{Pk}(x_2, y_2)$), occur

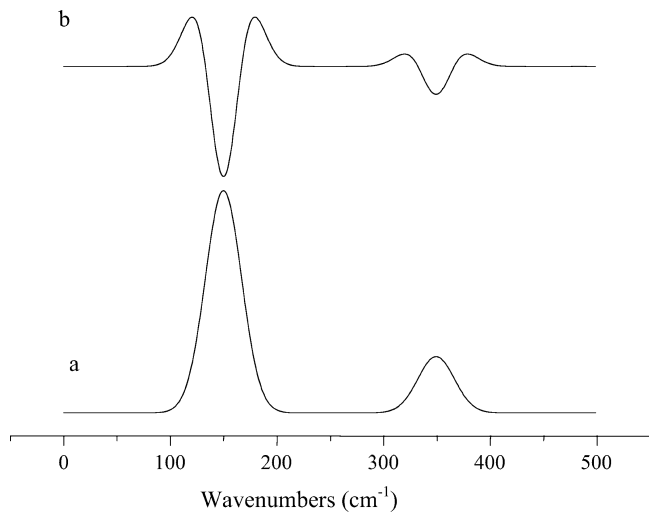


Figure 7. 1D spectra of first solution in Table 1 of the model system: (a) mixture of P, Q, U, and V when variation of peak position is allowed due to intermolecular interactions ($X_U = 152$, $X_V = 147$); (b) the second derivative spectrum of (a) (characteristic peaks of U and V are not visible).

in domain I of synchronous and asynchronous 2D spectra. The absolute intensities of the positive and negative peak are the same. A vector from negative peak to positive peak in a cross peak cluster can be defined. The directions of the vectors could be characterized by θ_{syn} and θ_{asyn} , the angle between the vectors and the positive x axis in synchronous and asynchronous spectra, respectively. The two angles as marked in each 2D spectrum in Figures 8 and 9 can be used to reveal qualitative variation of the peak positions of U and V. In addition, the relationship between $\Delta X_Q/\Delta X_P$ and θ_{syn} exhibits a function similar to $y = \tan(x)$, as shown in Figure 10a, while the relationship between $\Delta X_Q/\Delta X_P$ and θ_{asyn} exhibits a function similar to $y = -\tan(x)$, as shown in Figure 10b. Thus, the value of $\Delta X_Q/\Delta X_P$ could also be determined according to value of θ_{syn} and θ_{asyn} .

The spectral behaviors in domain II of asynchronous spectra are only related to the variation of X_P and X_U . If $\Delta X_P = 0$, no cross peak appears in domain II. If $\Delta X_P \neq 0$, a pair of cross peaks ($Pk(a,b)$, $Pk(b,a)$) which are antisymmetric about the diagonal line occur in domain II. The negative one appears on the left-upper side when $\Delta X_P > 0$, while it appears on the right-down side when $\Delta X_P < 0$. Furthermore, a good linear

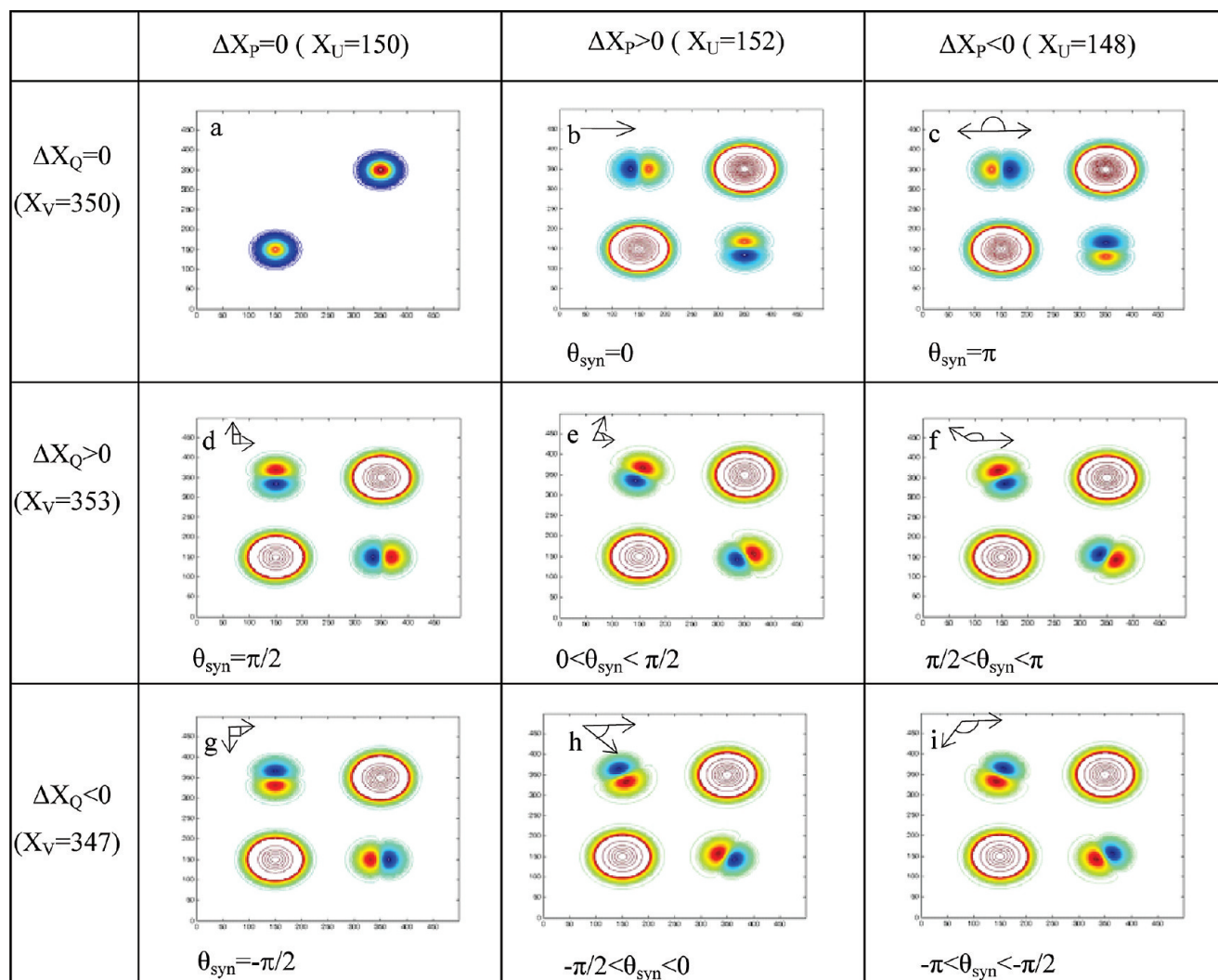


Figure 8. 2D synchronous spectra of the model system obtained as a consequence of variation of peak positions and the corresponding directions of the vectors θ_{syn} .

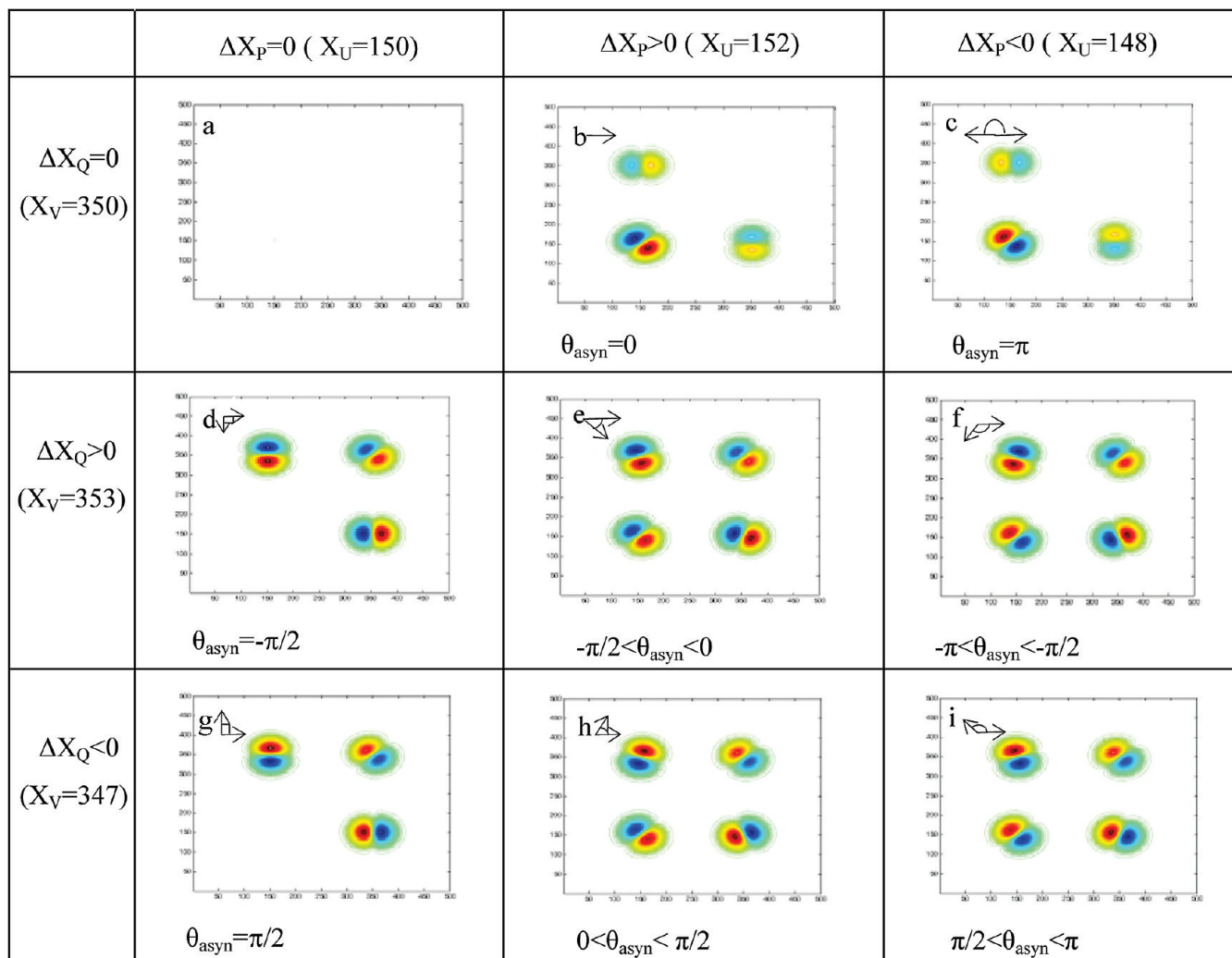


Figure 9. 2D asynchronous spectra of the model system obtained as a consequence of variation of peak positions and the corresponding directions of the vectors θ_{asyn} .

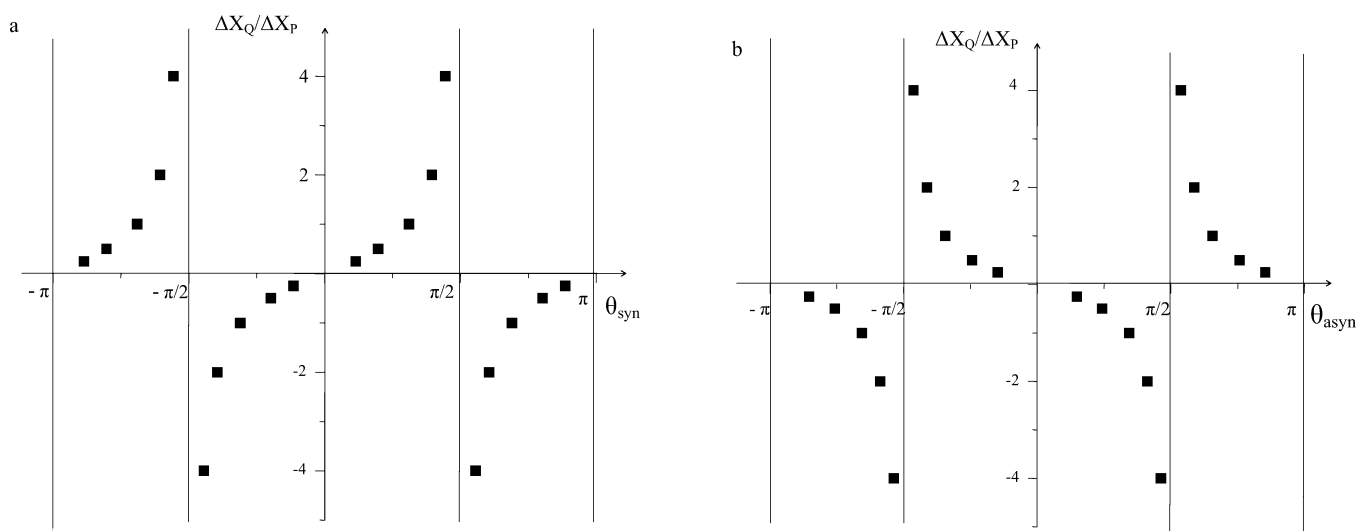


Figure 10. Relationships between θ_{syn} and θ_{asyn} and the value of $\Delta X_Q/\Delta X_P$: (a) $\Delta X_Q/\Delta X_P$ and θ_{syn} with a function similar to $y = \tan x$; (b) $\Delta X_Q/\Delta X_P$ and θ_{asyn} with a function similar to $y = -\tan x$.

relationship could be obtained between ΔX_p and the value of $a+b$ as illustrated in Figure 11. That is to say, ΔX_p could be

determined by the peak positions of the two cross peaks in domain II according to the following function:

$$\Delta X_P = 2X_P - (a + b)$$

The spectral behaviors of domain III, which are only related to the variation of X_Q and X_V , are very similar to that of domain II. We assume that the peak positions of the double cross peaks locate at (c, d) and (d, c). The value of ΔX_Q could also be obtained by the following function:

$$\Delta X_Q = 2X_Q - (c + d)$$

Further investigation demonstrates that a one-to-one correspondence relationship can also be established between the spectra patterns in synchronous as well as asynchronous spectra and the types of variation of peak positions of U and V. Thus, the variation of peak positions of U and V can be determined by different patterns shown in Figure 7.

(3) Effect of the Variation in Absorptivity of U and V. In this case, the peak positions and the bandwidths of U and V are the same as those of P and Q, while the absorptivities of U and V are allowed to be changed. The spectral variable for P, Q, U, and V are summarized in Table 8. The difference in the absorptivity between P and U is denoted as $\Delta \varepsilon_P$:

$$\Delta \varepsilon_P = \varepsilon_U - \varepsilon_P$$

Similarly, the difference in the peak position between Q and V is denoted as $\Delta \varepsilon_Q$:

$$\Delta \varepsilon_Q = \varepsilon_V - \varepsilon_Q$$

Complete overlapping occurs between the characteristic peaks of P and U in the resultant spectra, because the peak position and bandwidth are the same. As a typical example, ε_U is set to be 10% larger than ε_P and about 10% of P is converted into U because of intermolecular interactions between P and Q. Therefore, the intensity of the characteristic peak of P/U mixture is about 1% larger than the peak of pure P. As shown in Figure 12, the difference between the spectrum of P/Q mixture with intermolecular interactions and that without intermolecular

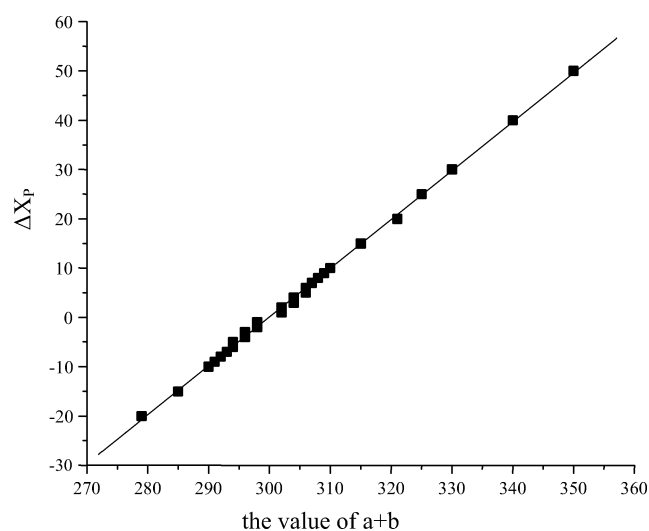


Figure 11. Relationship between ΔX_P and the value of $a + b$, a good linear relationship could be obtained with the function: $\Delta X_P = -(a + b) + 300$.

TABLE 8: Spectral Variables of the Chemical Species P, Q, U, and V in the Model System Where the Absorptivities of U and V (ε_U and ε_V) Are Variable

spectral variable	peak position (cm ⁻¹)	bandwidth (cm ⁻¹)	absorptivity
P	150	20	1.0
Q	350	20	1.0
U	150	20	ε_U
V	350	20	ε_V

interactions (achieved by setting the equilibrium constant K zero) are too subtle to be visualized.

However, the cross peaks in 2D synchronous and 2D asynchronous spectra generated by using the DOSD approach once again manages to be used to identify the existence of U or V caused by intermolecular interactions. Typical synchronous and asynchronous spectra resulting from the variation of absorptivities are shown in Figure 13. A single cross peak at (150, 350) appears in domain I of both synchronous and asynchronous spectra. The signs and intensities of the cross peaks are related to the variation of ε_U and ε_V . No peak appears in domains II and III of asynchronous spectra. The spectral patterns in synchronous and asynchronous can be classified into four types as far as the signs of cross peaks in synchronous and asynchronous spectra are concerned. However, the combination of the signs of $\Delta \varepsilon_P$ and $\Delta \varepsilon_Q$ can be divided into eight cases ($\Delta \varepsilon_P > 0$ and $\Delta \varepsilon_Q = 0$; $\Delta \varepsilon_P < 0$ and $\Delta \varepsilon_Q = 0$; $\Delta \varepsilon_P = 0$ and $\Delta \varepsilon_Q > 0$; $\Delta \varepsilon_P = 0$ and $\Delta \varepsilon_Q < 0$; $\Delta \varepsilon_P > 0$ and $\Delta \varepsilon_Q > 0$; $\Delta \varepsilon_P > 0$ and $\Delta \varepsilon_Q < 0$; $\Delta \varepsilon_P < 0$ and $\Delta \varepsilon_Q < 0$; $\Delta \varepsilon_P < 0$ and $\Delta \varepsilon_Q > 0$).). Therefore, it is not possible to obtain the one to one corresponding relationships between the patterns of synchronous and asynchronous spectra and the variation of $\Delta \varepsilon_P$ and $\Delta \varepsilon_Q$. However, partial information of $\Delta \varepsilon_P$ and $\Delta \varepsilon_Q$ can be obtained.

Figure 14 shows a 2D map of the intensities of the cross peaks in 2D synchronous and asynchronous spectra (I_{syn} and I_{asyn} , respectively) as a function of $\Delta \varepsilon_P$ and $\Delta \varepsilon_Q$. The $\Delta \varepsilon_P \sim \Delta \varepsilon_Q$ plane is divided into four parts according to the combination of the signs of the cross peaks in synchronous and asynchronous spectra. We notice that the origin of the $\Delta \varepsilon_P \sim \Delta \varepsilon_Q$ plane is just the cross-section of the two border lines ($I_{\text{syn}} = 0$ and $I_{\text{asyn}} = 0$). We have investigated chemical system with different equilibrium constant and the results are quite similar to that shown in Figure 14. Thus a rule to judge variation of $\Delta \varepsilon_P$ and $\Delta \varepsilon_Q$

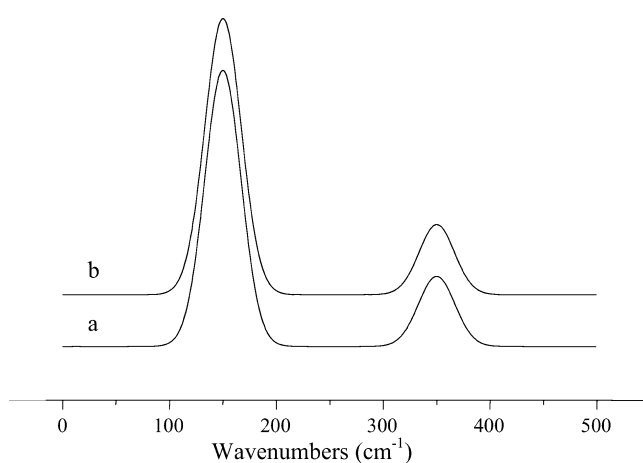


Figure 12. 1D spectra of first solution in Table 1 of the model system: (a) mixture of P, Q, U, and V when absorptivity variation is allowed due to intermolecular interactions ($\varepsilon_U = 1.1$, $\varepsilon_V = 0.9$); (b) no intermolecular interaction achieved by setting the equilibrium constant K to zero.

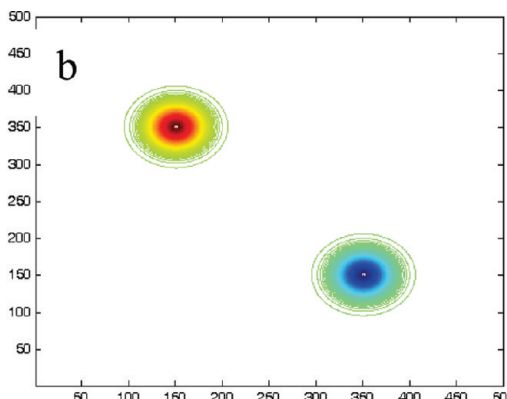
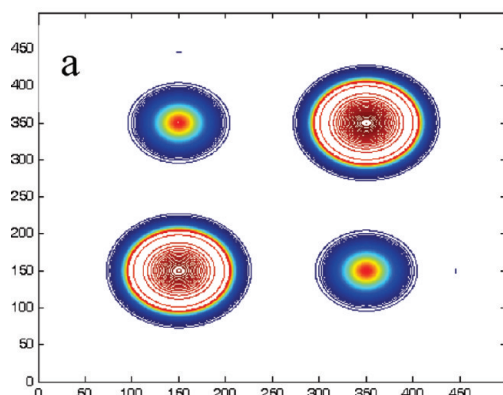


Figure 13. Patterns of the cross peaks in (a) synchronous and (b) asynchronous spectra as a consequence of variation of absorptivities ($\varepsilon_U = 1.10$, $\varepsilon_V = 1.05$).

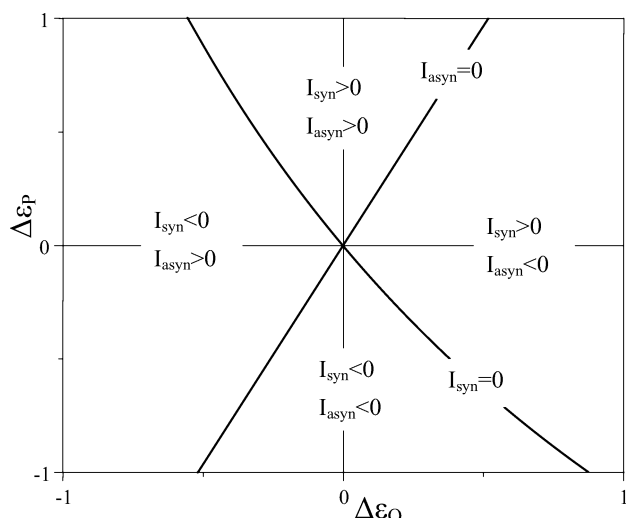


Figure 14. 2D map of the intensities of the cross peaks in 2D synchronous and asynchronous spectra (I_{syn} and I_{asyn}) as a function of $\Delta \varepsilon_p$ and $\Delta \varepsilon_Q$, only the zero intensity lines are marked ($I_{\text{syn}} = 0$, $I_{\text{asyn}} = 0$).

TABLE 9: Relationship between the Sign of Cross Peaks in Synchronous and Asynchronous Spectra and the Corresponding Variation of ε_U and ε_V

sign of the cross peak in domain I			
synchronous spectra	asynchronous spectra	corresponding variation of ε_U and ε_V	
1 positive	positive	$\Delta \varepsilon_p > 0$	
2 positive	negative	$\Delta \varepsilon_Q > 0$	
3 negative	negative	$\Delta \varepsilon_p < 0$	
4 negative	positive	$\Delta \varepsilon_Q < 0$	

according to the combination of the signs of synchronous and asynchronous spectra can be summarized as shown in Table 9.

3. Example for Application of the DOSD Method in the Real Chemical System. The benzene–iodine complex has been the subject of many experimental and theoretical studies for near sixty years.^{37–41} In 1949, Benesi and Hildebrand³⁷ observed an absorption band in UV region that could not be attributed to the benzene monomer nor to the iodine molecule. They concluded that this absorption was a result of a charge-transfer (CT) transition. The benzene acts as an electron donor, and the iodine as an acceptor. Although this model offers an excellent explanation for the charge-transfer bands observed in electronic spectra, it was later shown that charge-transfer interactions are not a very important contribution to the ground-state interaction energy. Other contributions (polarization, electrostatic, and dispersion) were responsible

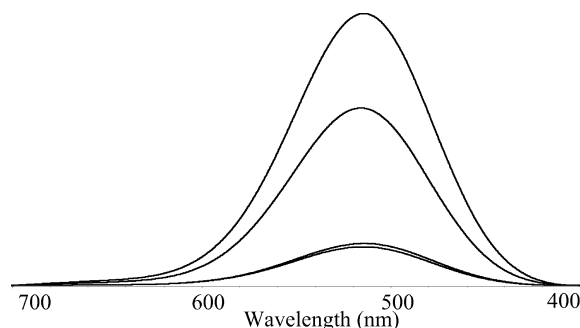


Figure 15. 1D UV–vis spectra of the I_2 –benzene/CCl₄ solutions used for generating 2D correlated spectra by the DOSD approach.

for the stability of the complex, and ab initio calculations showed that dispersion was the most important contribution.^{42,43} The above reports suggest that benzene–iodine may be used to test the effectiveness of the DOSD approach. Therefore, we select the I₂/benzene/CCl₄ system as a real chemical system and a preliminary investigation on intermolecular interaction between I₂ and benzene were performed. In the I₂/benzene/CCl₄ system, iodine shows a characteristic peak around 516 nm corresponding to the electronic transition from $B^3\Pi_{\text{ou}}^+$ and $X^1\Sigma_g^+$ in UV–vis spectra while benzene has no absorbance between 400 and 700 nm. Additionally, iodine does not show any absorbance above 1000 cm⁻¹ in FT-IR spectra. The overlapping problem of characteristic peaks of two solutes can be avoided. C–H stretching bands in the 3100–3000 cm⁻¹ region and an overtone band around 1957 cm⁻¹ of benzene do not overlap with any absorption band of the solvent CCl₄. Thus, we can construct 2D-FT-IR–UV–vis heterogeneous 2D spectra by using the DOSD approach to characterize the intermolecular interactions between I₂ and benzene in CCl₄.

In the literature, the intermolecular interaction between I₂ and benzene are characterized by charge-transfer bands around 280 nm, which is very sensitive to intermolecular interactions. In our work, experimental evidence of an intermolecular interaction can be obtained from those bands that do not exhibit significant spectral variation under the occurrence of intermolecular interactions.

UV–vis spectra and FT-IR spectra of the four solutions are shown in Figures 15 and 16, respectively. Except for changes in intensities related to the variation of initial concentrations of benzene and I₂, no significant spectral changes are observed. The resultant 2D spectra are plotted in Figures 17 and 18. The observation of cross peaks in both synchronous and asynchronous 2D spectra generated by using the DOSD approach demonstrates that intermolecular interactions do occur between benzene and I₂ in CCl₄ solutions.

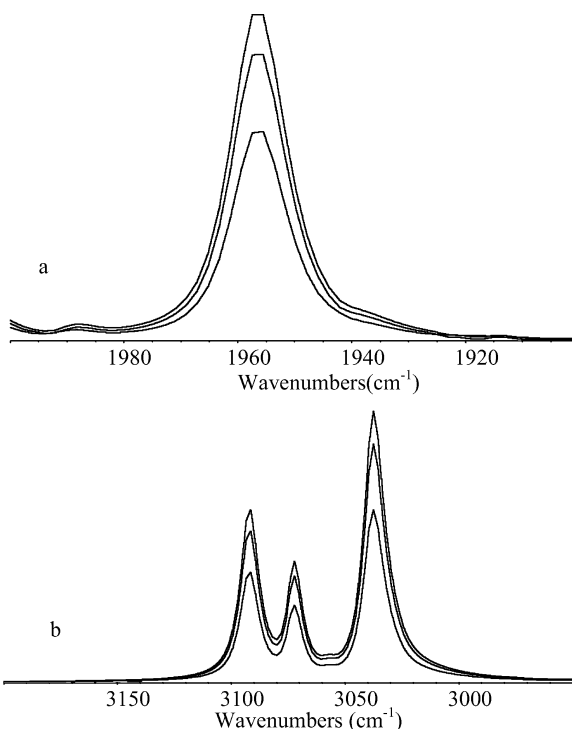


Figure 16. 1D FT-IR spectra of the I_2 -benzene/CCl₄ solutions used for generating 2D correlated spectra by the DOSD approach: (a) 2000–1900 cm⁻¹, the overtone region; (b) 3200–2950 cm⁻¹, the C–H stretching band region.

Principal component analysis was carried on the four UV–FT-IR joint spectra used to generate the 2D synchronous spectra. Three nonzero eigenvalues were obtained, confirming the formation of the benzene–iodine complex in the solutions. The results also demonstrate the coexistence of free benzene, I₂, and benzene–iodine complex in the solutions. Severe band-overlapping occurs on the corresponding characteristic bands, which can be revealed by the spectral pattern in both synchronous and asynchronous 2D spectra. A pair of horizontal cross peaks (one positive cross peak and one negative peak) appears in domain I of both synchronous and asynchronous spectra shown in Figure 17. Similarly, three pairs of cross peaks appear in domain I of both synchronous and asynchronous spectra in Figure 18. A pair of strong cross peaks that is antisymmetric about the diagonal appears in domain II of the 2D asynchronous spectra in Figures 17b and 18b. There is almost no cross peak in domain III of Figure 17b, suggesting that there is almost no band shift or variation in the bandwidth of the 1957 cm⁻¹ band. However, weak cross peaks appear domain III of asynchronous spectra in Figure 18b, implying a very slight band shift occurs in the C–H stretching band of benzene. Since the band shift of the C–H stretching band of benzene is much smaller than that of I₂, the three pairs of cross peaks in domain I are almost horizontal, as shown in Figure 18a,b. The patterns of 2D synchronous and asynchronous spectra in Figures 17 and 18 are similar to those in Figures 8c and 9c obtained in the simulation study. That is to say, the spectral patterns shown in Figures 17 and 18 suggest the characteristic peak of I₂ molecules undergo a blue shift in the UV–vis spectra upon involving in intermolecular interaction. This result is supported by the following fact reported in the literature:³⁷ In comparison with UV–vis spectra of I₂ dissolved in CCl₄, the characteristic peak underwent a blue shift when I₂ was dissolved in benzene. In our system, CCl₄ plays a dilution

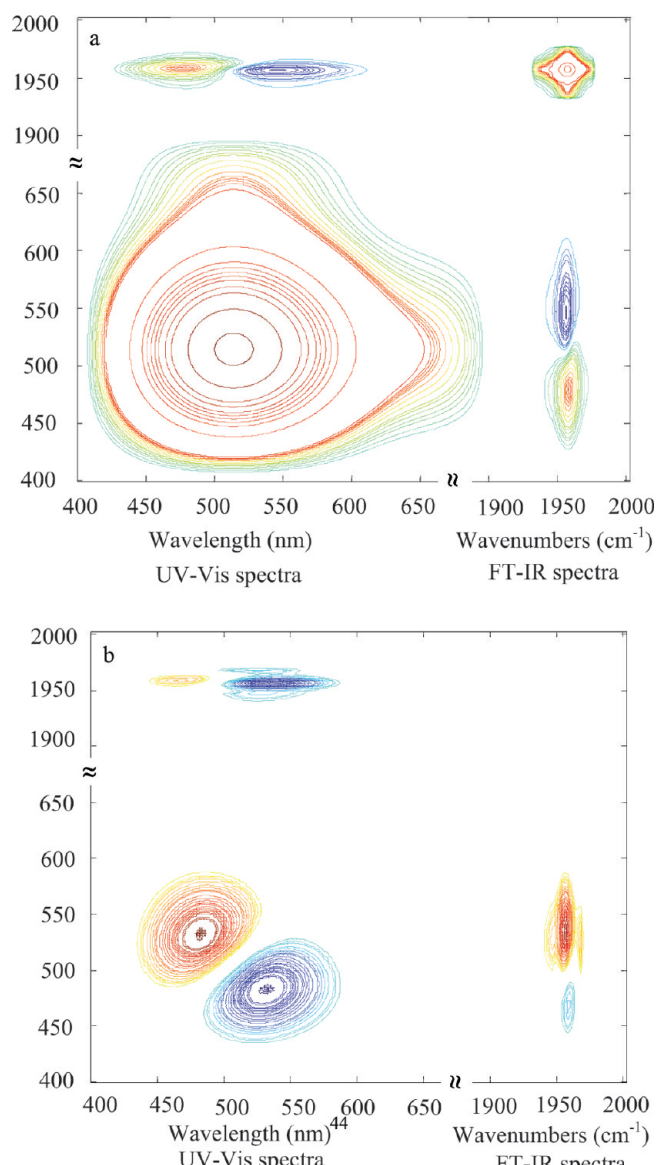


Figure 17. 2D synchronous (a) and asynchronous (b) correlation spectra according to the UV–vis spectra and IR spectra (2000–1900 cm⁻¹ region) of the benzene/I₂/CCl₄ system.

role. Thus it is quite difficult to observe spectral variations caused by intermolecular interaction between I₂ and benzene in 1D spectra since the concentration of I₂–benzene complex is rather low. Nevertheless, the 2D spectra generated by using the DOSD approach are sensitive enough to reveal such subtle spectral variations. Another notable feature in 2D spectra is that C–H stretching band of benzene may exhibit slight blue shift upon binding with I₂. The above results indicate that the intermolecular interaction between benzene and iodine affect the relative energy levels of $B^3\Pi_{ou}^+$ and $X^1\Sigma_g^+$ states. On the other hand, the intermolecular interaction may also influence the peak position of C–H stretching bands slightly.

Conclusion

In this paper, the DOSD approach is developed to remove the interfering portion from the cross peaks in both 2D synchronous and asynchronous spectra. Thus, combination of the spectral information from 2D synchronous and asynchronous spectra can be utilized to characterize intermolecular interactions. Computer simulation demonstrates

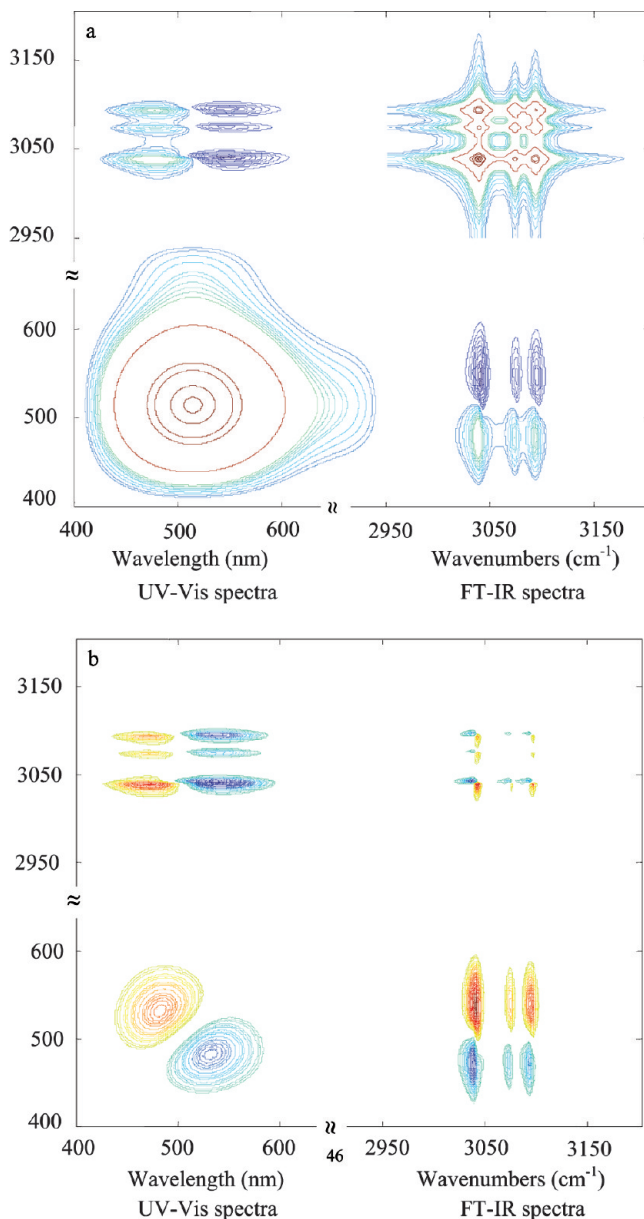


Figure 18. 2D synchronous (a) and asynchronous (b) correlation spectra according to the UV-vis spectra and IR spectra ($3200\text{--}2950\text{ cm}^{-1}$ region) of the benzene/ I_2/CCl_4 system.

that distinct 2D spectral patterns produced by the DOSD approach reflect subtle variations in bandwidths, peak positions, and absorptivities of characteristic bands of solutes caused by intermolecular interactions, which are hardly detected due to the band overlapping problem. The applicability of the DOSD approach in the real chemical system has also been proved by the $I_2/\text{benzene}/CCl_4$ system. It is worth noting that the DOSD approach is applicable for many kinds of intermolecular interactions. Therefore, the DOSD approach may enhance our understanding on the nature of intermolecular interactions by revealing subtle spectral variations of the characteristic bands of substances involved. More work concerning investigation on the 2D spectral patterns due to some complicated 1D spectral variation in simulation study and experiments on real chemical systems is in progress.

Acknowledgment. This project is supported by the National Natural Science Foundation of China (NSFC50673005, NSFC50403026, NSFC50973003, and NSFC20671007).

Supporting Information Available: Text giving the results of the FT-IR spectra of benzene/ CCl_4 solutions and UV-vis spectra of iodine/ CCl_4 solutions. Figures S1–S5 showing the relationships between the concentrations of two solutes and the absorbance of corresponding characteristic peaks in UV-vis spectra and FT-IR spectra. This material is available free of charge via the Internet at <http://pubs.acs.org>.

References and Notes

- (1) Noda, I. *J. Am. Chem. Soc.* **1989**, *111*, 8116.
- (2) Noda, I. *Appl. Spectrosc.* **1990**, *44*, 550.
- (3) Noda, I. *Appl. Spectrosc.* **1993**, *47*, 1329.
- (4) Noda, I. *Appl. Spectrosc.* **2000**, *54*, 994.
- (5) Sato, H.; Mori, K.; Murakami, R.; Ando, Y.; Takahashi, I.; Zhang, J. M.; Terauchi, H.; Hirose, F.; Senda, K.; Tashiro, K.; Noda, I.; Ozaki, Y. *Macromolecules* **2006**, *39*, 1525.
- (6) Peng, Y.; Wu, P. Y.; Siesler, H. W. *Biomacromolecules* **2003**, *4*, 1041.
- (7) Zhang, J. M.; Sato, H.; Tsuji, H.; Noda, I.; Ozaki, Y. *Macromolecules* **2005**, *38*, 1822.
- (8) Wu, Y. Q.; Jiang, J. H.; Ozaki, Y. *J. Phys. Chem. A* **2002**, *106*, 2422.
- (9) Wu, Y. Q.; Murayama, K.; Ozaki, Y. *J. Phys. Chem. B* **2001**, *105*, 6251.
- (10) Jung, Y. M.; Kim, S. B.; Noda, I. *Appl. Spectrosc.* **2003**, *57*, 557.
- (11) Czarnik-Matusewicz, B.; Murayama, K.; Wu, Y. Q.; Ozaki, Y. *J. Phys. Chem. B* **2000**, *104*, 7803.
- (12) Czarnecki, M. A.; Czarnik-Matusewicz, B.; Ozaki, Y.; Iwahashi, M. *J. Phys. Chem. A* **2000**, *104*, 4906.
- (13) Morita, S.; Shinzawa, H.; Noda, I.; Ozaki, Y. *Appl. Spectrosc.* **2006**, *60*, 398.
- (14) He, Y.; Wang, G. F.; Cox, J.; Geng, L. *Anal. Chem.* **2001**, *73*, 2302.
- (15) Wang, G.; Gao, Y.; Geng, L. *J. Phys. Chem. B* **2006**, *110*, 8506.
- (16) Noda, I.; Marcott, C. *J. Phys. Chem. A* **2002**, *106*, 3371.
- (17) Yu, Z. W.; Noda, I. *Appl. Spectrosc.* **2003**, *57*, 164.
- (18) Jung, Y. M.; Czarnik-Matusewicz, B.; Ozaki, Y. *J. Phys. Chem. B* **2000**, *104*, 7812.
- (19) Zhao, W.; Murdoch, K. M.; Besemann, D. M.; Wright, J. C. *Appl. Spectrosc.* **2000**, *54*, 1000.
- (20) Awichi, A.; Tee, E. M.; Srikanthan, G.; Zhao, W. *Appl. Spectrosc.* **2002**, *56*, 897.
- (21) Kang, N.; Xu, Y. Z.; Cai, Y. L.; Li, W. H.; Weng, S. F.; Feng, W.; He, L. T.; Xu, D. F.; Wu, J. G.; Xu, G. X. *J. Mol. Struct.* **2001**, *562*, 19.
- (22) Yu, Z. W.; Chen, L.; Sun, S. Q.; Noda, I. *J. Phys. Chem. A* **2002**, *106*, 6683.
- (23) Ren, Y. Z.; Shimoyama, M.; Ninomiya, T.; Matsukawa, K.; Inoue, H.; Noda, I.; Ozaki, Y. *J. Phys. Chem. B* **1999**, *103*, 6475.
- (24) Heo, K. Y.; Yoon, J. W.; Jin, K. S.; Jin, S. W.; Sato, H.; Ozaki, Y. H.; Satkowski, M. M.; Noda, I.; Ree, M. *J. Phys. Chem. B* **2008**, *112*, 4571.
- (25) Qi, J.; Li, H. Z.; Huang, K.; Chen, H. H.; Liu, S. X.; Yang, L. M.; Zhao, Y.; Zhang, C. F.; Li, W. H.; Wu, J. G.; Xu, D. F.; Xu, Y. Z.; Noda, I. *Appl. Spectrosc.* **2007**, *61*, 1359.
- (26) Chen, J.; Zhang, C.; Li, H.; Liu, Y.; Li, W.; Xu, Y.; Wu, J.; Noda, I. *J. Mol. Struct.* **2008**, *883*, 129.
- (27) Mehl, G. H.; Goodby, J. W. *Angew. Chem., Int. Ed.* **1996**, *35*, 2641.
- (28) Dey, S.; Adhikari, A.; Mandal, U.; Ghosh, S.; Bhattacharyya, K. *J. Phys. Chem. B* **2008**, *112*, 5020.
- (29) Chi, L. F.; Jacobi, S.; Anczykowski, B.; Overs, M.; Schafer, H. J.; Fuchs, H. *Adv. Mater.* **2000**, *12*, 25.
- (30) Bernardi, A.; Arosio, D.; Potenza, D.; Sanchez-Medina, I.; Mari, S.; Canada, F. J.; Jimenez-Barbero, J. *Chem.-Eur. J.* **2004**, *10*, 4395.
- (31) Mandal, U.; Adhikari, A.; Dey, S.; Ghosh, S.; Bhattacharyya, K. *J. Phys. Chem. B* **2007**, *111*, 5896.
- (32) Sahu, K.; Roy, D.; Mondal, S. K.; Karmakar, R.; Bhattacharyya, K. *Chem. Phys. Lett.* **2005**, *404*, 341.
- (33) Tschierske, C. *Angew. Chem., Int. Ed.* **2000**, *39*, 2454.
- (34) Hansen, D. F.; Hass, M. A. S.; Christensen, H. M.; Ulstrup, J.; Led, J. J. *J. Am. Chem. Soc.* **2003**, *125*, 6858.
- (35) Nakash, M.; Goldvaser, M. *J. Am. Chem. Soc.* **2004**, *126*, 3436.
- (36) Qian, W.; Krimm, S. *J. Phys. Chem. A* **1997**, *101*, 5825.
- (37) Benesi, H. A.; Hildebrand, J. H. *J. Am. Chem. Soc.* **1949**, *71*, 2703.
- (38) Fredin, L.; Nelander, B. *J. Am. Chem. Soc.* **1974**, *96*, 1672.
- (39) Grozema, F. C.; Zijlstra, R. W. J.; Swart, M.; Van Duijnen, P. Th. *Int. J. Quantum Chem.* **1999**, *75*, 709.
- (40) Kiviniemi, T.; Hulkko, E.; Kiljunen, T.; Pettersson, M. *J. Phys. Chem. A* **2008**, *112*, 5025.
- (41) Weng, K.-F.; Shi, Y.; Zheng, X.; Phillips, D. L. *J. Phys. Chem. A* **2006**, *110*, 851.
- (42) Mantione, M.-J. *Theo Chim Acta* **1968**, *11*, 119.
- (43) Hanna, M. W.; Lippert, J. In *Molecular Complexes*; Foster, R., Eds.; Elek Science: London, 1973.